LARGE-SCALE ATMOSPHERIC FORCING INFLUENCING THE LONG TERM VARIABILITY OF MEDITERRANEAN HEAT AND FRESHWATER BUDGETS: CLIMATIC INDICES

Francisco Criado-Aldeanueva[(1)], F. Javier Soto-Navarro[(1)], Jesús García-Lafuente[(1)]

(1) Physical Oceanography Group, Department of Applied Physics II, University of Málaga, Málaga, Spain.

Corresponding author:

Francisco Criado Aldeanueva

Dpto. Física Aplicada II, Universidad de Málaga

29071 Málaga, Spain

Tel.: +34 952 132849

fcaldeanueva@ctima.uma.es

LARGE-SCALE ATMOSPHERIC FORCING INFLUENCING THE LONG TERM VARIABILITY OF MEDITERRANEAN HEAT AND FRESHWATER BUDGETS: CLIMATIC INDICES

ABSTRACT: Interannual to interdecadal precipitation (P), evaporation (E), freshwater budget (E-P) and air-sea net heat flux (Q) have been correlated with the North Atlantic Oscillation (NAO), East Atlantic (EA), East Atlantic – West Russia (EA-WR) and Mediterranean Oscillation (MO) climatic indices to explore the influence of atmospheric forcing in the Mediterranean freshwater and heat budgets variability. The effect of MO pattern has similarities with that of NAO but MO influence is more intense: on annual basis, MO index gives the highest correlation with all the variables considered and, during its negative phase, it exerts a stronger influence than NAO and is associated with higher P and, especially, enhanced evaporative losses in the Levantine sub-basin. EA pattern does not significantly affect P in the Mediterranean but a high correlation is found for E and Q from 1979. EA-WR mode plays a significant role in annual net heat flux since variations in its sign have the potential to induce see-saw variations in the heat budgets of the eastern and western sub-basins, as previously found by Josey et al. (2011) for wintertime.

Keywords: Heat and freshwater budgets, long-term variability, atmospheric forcing, climatic indices, Mediterranean Sea.

1.- INTRODUCTION

The Mediterranean Sea (Figure 1), a marginal basin located across a dynamic border that separates two different climatic regions (Europe and North Africa), extends over 3000 km in longitude and over 1500 km in latitude with an area of $2.5 \cdot 10^{12}$ m^2 and communicates with the Atlantic Ocean through the Strait of Gibraltar and with the Black Sea through the Turkish Bosphorus and Dardanelles Straits. Semi-enclosed basins such as the Mediterranean are suitable for the characterisation of heat and water fluxes since they make a basin budget closure feasible. As evaporation (E) exceeds precipitation (P) and river runoff (R), inflow from Atlantic through the Strait of Gibraltar is necessary to balance the water and salt budgets.

--------------------------------Approximate location of Figure 1--------------------------------

A great number of studies have dealt with the Mediterranean heat (Bethoux, 1979; Bunker et al., 1982; May, 1986; Garrett et al., 1993; Gilman and Garrett, 1994; Castellari et al., 1998; Matsoukas et al., 2005; Ruiz et al., 2008; Criado-Aldeanueva et al., 2012) and water (Bethoux, 1979; Peixoto et al., 1982; Bryden and Kinder, 1991; Harzallah et al., 1993; Gilman and Garrett, 1994; Castellari et al., 1998; Angelucci et al., 1998; Béthoux and Gentili, 1999; Boukthir and Barnier, 2000; Mariotti et al., 2002; Mariotti, 2010; Romanou et al., 2010; Criado-Aldeanueva et al., 2012) budgets but only in the recentmost ones, which use longer datasets, the attention focused on the interannual variability and its forcing mechanisms. For instance, Criado-Aldeanueva et al. (2012) report three different periods in the precipitation and evaporation anomalies: from early 50s to late 60s, a positive trend is observed that changes to negative until late

80s when it changes sign again. This variability also reflects in the net heat flux exchanged between the ocean and atmosphere and suggests a 40-year period multi-decadal oscillation related to long-term atmospheric forcing that needs further investigation.

Climatic indices that represent modes of atmospheric variability provide an integrated measure of weather linked more to the overall physical variability of the system than to any individual local variable. Among these indices, the North Atlantic Oscillation (NAO) is one of the most prominent modes of the northern hemisphere climate variability (Walker and Bliss, 1932; van Loon and Rogers, 1978; Barnston and Livezey 1987; see Hurrell et al., 2003 for a recent review). It consists of a dipole of the sea level pressure over the North Atlantic-European region with one centre reflecting the Iceland low and the other the Azores high. The positive phase of the NAO (Figure 2A) is associated with higher than average sea level pressure (SLPA) over most parts of Europe and the Mediterranean Sea. The intensification of the Azores High and the deepening of the Icelandic Low during this phase strengthens and modifies the orientation of westerlies and associated storm-track activity and leads to drier conditions in southern Europe (south of 45ºN) and the Mediterranean and wetter in northern Europe (Walker and Bliss 1932; van Loon and Rogers 1978; Rogers and van Loon 1979; Hurrell 1995; Serreze et al., 1997; Dai et al., 1997; Mariotti et al., 2002; Mariotti and Arkin, 2007). Opposite conditions prevail during the negative phase (Figure 2B), with lower than average SLPA over south Europe and the Mediterranean that lead to higher precipitation in these areas.

---------------------------------Approximate location of Figure 2---------------------------------

The influence of large-scale atmospheric circulation on the climate variability over the Mediterranean region has also been addressed in terms of other teleconnection patterns such as the East-Atlantic (EA), the East Atlantic – West Russia (EA-WR) or the Scandinavian (SCAN) patterns (Josey et al., 2011; Papadopoulos et al., 2012a, b). The positive phase of the EA pattern (Figure 2C) is dominated by a broad region of anomalously low pressure centred approximately midway of the two centres of the NAO (Josey and Marsh, 2005) that gives rise to strong cyclonic wind forcing of the North Atlantic around this location. In its negative state (Figure 2D), it produces a relatively strong pressure gradient in the western Mediterranean which can potentially generate a cold northerly airflow and enhanced heat loss in this region (Josey et al., 2011). The EA-WR pattern (Figure 2E-F) exhibits anomalously high (low) pressure over the North Sea flanked by low (high) pressure centres over West Russia and over the western North Atlantic at 45-55ºN. Positive phases of EA-WR favour northerlies over eastern Mediterranean and southerlies over western Mediterranean. The SCAN pattern (not shown) produces weak variations in the SLPA field and plays a minor role in the large-scale atmospheric forcing over the Mediterranean (Josey et al, 2011; Papadopoulos et al., 2012a).

Conte et al (1989) suggested the possible existence of a Mediterranean Oscillation (MO) associated with dipolar behaviour of the atmosphere in the area between the western and eastern Mediterranean. Differences in temperature, precipitation, circulation and other parameters between both basins were attributed to this MO (Conte et al., 1989; Kutiel et al., 1996; Maheras et al., 1999, Supic et al., 2004) and an index to measure the intensity of this dipole-like behaviour was proposed as the normalised 500 hPa height difference anomalies between Algiers (36.4ºN, 3.1ºE) and Cairo (30.1ºN, 31.4ºE) (Conte et al., 1989). A second version of the index can be calculated based on normalized sea level pressure differences between Gibraltar northern frontier (36.1ºN, 5.3ºW) and Lod Airport Israel (32.0ºN, 34.5ºE) (Palutikof, 2003, available at http://www.cru.uea.ac.uk/cru/data/moi/) and, more recently Papadopoulos et al. (2012a, b) introduced the Mediterranean index as the sea level pressure difference between south France (45ºN, 5ºE) and Levantine Sea (35ºN, 30ºE). Suselj and Bergant (2006) proposed a MO index definition based on EOF analysis of SLPA fields over an extended Mediterranean region and Gomis et al. (2006) also adopted this definition to study its influence in the flow exchange through Gibraltar. For the reasons given in section 2, we have adopted this EOF-based approach to the MO index for this research.

In contrast to NAO, that has been extensively studied, and the other atmospheric indices, only a few previous works focus on the MO index (especially during winter) and more research is required on this topic. This work adds some of this research by exploring MO influence in annual heat and freshwater budgets in comparison with the other teleconnection patterns. To this aim, we correlate interannual to interdecadal precipitation, evaporation, freshwater budget (E-P) and net heat flux with several atmospheric climatic indices (NAO, EA, EA-WR and MO) and analyse the relative importance of their positive and negative phases in the variables. The work is organised as follows: section 2 describes the data and methodology; section 3 presents and discuss the results both from a regional and global approach and finally section 4 summarises the conclusions.

2.- DATA AND METHODOLOGY

Since there is no unique way to describe the spatial structure of the low-frequency atmospheric modes of variability, it follows that there is no universally accepted index to describe the temporal evolution of the phenomenon. Climatic indices have been traditionally derived either from the simple difference in surface pressure anomalies or some other climate variable between various locations (e.g., Conte et al., 1989; Palutikof, 2003; Papadopoulos et al., 2012a, b for MO index; Rogers, 1984;; Hurrell, 1995; Jones et al., 1997; Slonosky and Yiou, 2001; Jones et al., 2003 for a comparison between several station-based NAO indices) or from the Principal Components (PC) time series of the leading Empirical Orthogonal Function (EOF) of sea level pressure or some other climate variable (Suselj and Bergant, 2006; Gomis et al., 2006 for MO index; see Hurrell and Deser, 2010 for a review of diverse NAO definitions). A widely employed analysis of the main modes of atmospheric variability is that carried out at the National Oceanic and Atmospheric Administration (NOAA) Climate Prediction Centre (CPC). They characterize the main modes through a rotated principal component analysis (Barnston and Livezey, 1987) of the observed monthly mean 500 mb height anomaly fields in the region 20ºN-90ºN and provide monthly index values for each mode (see details in http://www.cpc.ncep.noaa.gov/data/teledoc/teleindcalc.shtml. In this study, we have retrieved CPC monthly index values for the NAO, EA and EA-WR patterns.

A disadvantage of the station-based indices is that they are fixed in space and are significantly affected by small-scale and transient meteorological events that introduce noise (Trenberth, 1984; Hurrell and van Loon, 1997) whereas the PC time series approach is more optimal representation of the full spatial pattern (Hurrell and Deser, 2010). For this reason and for homogeneity with the other climatic indices, the MO pattern has been computed as the first EOF mode of normalised sea level pressure anomalies (from NCEP dataset) across the extended Mediterranean region (30ºW-40ºE in longitude, 30ºN-60ºN in latitude) which exhibits a single centre located over the central and western Mediterranean (not shown), fairly steady in all seasons. The MO index is then obtained as the corresponding time coefficients of the first EOF mode.

It is important to notice that NAO, EA and EA-WR can act independently as modes resulting from the same EOF analysis. MO shows some similarity with NAO, with higher (lower) than average SLPA over the Mediterranean during its positive (negative) phase (Figure 2G-H). On annual basis, correlation of MO index with the independent modes of low frequency variability is 0.57 with NAO and 0.43 with EA (no significant correlation is observed with EA-WR). Seasonally, summer (JAS) MO index is only significantly correlated with NAO ($r = 0.37$) whereas winter (JFM) MO index exhibits a similar correlation ($r \sim 0.33$) with the rest of the indices. Being aware that MO captures to a certain extent the influence of the other independent modes (mainly NAO) and hence cannot act independently from them, its potential to affect more intensely the variables over the Mediterranean Sea merits investigation.

Monthly means from January 1948 to February 2009 of precipitation, evaporation and surface heat fluxes (positive toward the atmosphere, the same as evaporation) have been retrieved from the National Center for Enviromental Prediction-National Center of Atmospheric Research (NCEP-NCAR) reanalysis project (NCEP hereinafter, Kalnay et al., 1996), which is run at T62 spectral resolution (approximately a grid size of

1.9ºx1.9º) with 28 sigma levels. Auxiliary data of monthly mean sea level pressure at 2.5ºx2.5º for the period 1948-2009 have also been retrieved from NCEP database. Uncertainties derived from the use of reanalysis have been studied by Mariotti et al. (2002), who showed that NCEP data exhibit good agreement when compared with observational P and E datasets at interannual to inter-decadal time scales in the Mediterranean area (except some discrepancies in E in the 80s and 90s). For comparison purposes, we have also analysed monthly data from ERA-Interim, the latest reanalysis dataset released by ECMWF (Berrisford et al., 2009) that focused on the data-rich period since 1979. At 1.5º horizontal resolution, it includes many model improvements, variational bias correction for satellite data and other improvements in data handling. ERA-Interim uses mostly the sets of observations acquired for ERA-40 supplemented by data for recentmost years from ECMWF operational archive. Reasonably good agreement has been observed between these two reanalysis datasets in their common period both in the seasonal cycles (not shown) and in the interannual variability (Figures 3-6E). Due to the longer time coverage provided by NCEP, results will focus on this dataset but comparisons with ERA-Interim will be also discussed.

Although the use of reanalysis allows the construction of homogeneous time series (both in time and space) and leads to a better representation of the basin-scale features, validation with observational datasets is desirable for robustness. For this reason, data from the Climate Prediction Centre Merged Analysis of Precipitation (CMAP, Xie and Arkin, 1996, 1997) have also been retrieved and analysed. This dataset gives estimation of monthly mean precipitation at 2.5° × 2.5° resolution for the period 1979–2009. The standard version consists of a merged analysis mainly based on gauge stations over land and satellite estimates over the ocean that matches reasonably well the reanalysis outputs in their common period especially in terms of interannual variability (Figure 3E), this reinforcing reliability of our results.

Linear correlation maps have been used to identify coupled patterns between the variables and the atmospheric indices. The statistical significance of the correlation has been computed by transforming the correlation matrix in a *t*-student distribution with N-2 degrees of freedom, where N is the number of element of the analysed time series. Time filtering into low and high frequency components is achieved using a 5-year running mean to take into account the long time scale effects of the indices. Composite analysis (in terms of anomalies respect the climatic mean over 1948-2009) has also been performed to highlight the differences between the positive and negative phases of the indices, defined as the upper and lower quartiles of the climatic indices time series over the period 1948-2009. Only the points where the results are statistically different from zero (according to a *t*-Student test at 95% significance) have been represented.

3.- RESULTS AND DISCUSSION

3.1.- Precipitation

Table 1 shows the correlation between precipitation and the climatic indices for the several datasets analysed. On annual basis, the MO index shows the highest (negative) correlation (*r* = 0.45 on average over 56% of the Mediterranean) with values up to -0.7 in the Aegean and northern Levantine sub-basins (Figure 3A). The correlation increases in winter (or if the entire rainy period, from October to March is considered), when P is generally linked to storm-track activity captured by atmospheric indices, with wide regions close to -0.6 (not shown). In summer, most of precipitation across the Mediterranean region is of convective origin and is poorly correlated with the large-scale atmospheric forcing. At decadal timescales (5-year running means), MO and NAO have a similar performance (r = 0.56 on average) and up to 80% of the basin (except the south-Ionian and westernmost areas) is significantly correlated (Figure 3B). EA and EA-WR exhibit lower correlation with P and only some isolated regions are sensitive to their effect (see Table 1). Correlation is rather similar for different datasets but fairly dependent of the period analysed (this making the 60-year NCEP time series the most reliable for long-term variability): if only the period from 1979 is considered (ERA-Interim, $NCEP_{79\text{-}09}$ and CMAP data), correlation between MO index and P is weaker in general since departure from both time series is evident, especially from 2000 but also in the 80s (Figure 3E).

--------------------------------Approximate location of Figure 3--------------------------------

--------------------------------Approximate location of Table 1---------------------------------

Negative correlation of P with NAO (and MO, see the similarity between their SLPA fields in Figure 2) is a well documented feature because its positive phase (stronger dipole) produces a SLPA field (Figure 2A) that strengthens and modifies the orientation of prevailing westerly winds and associated storm-track activity which cause dry anomalies in the Mediterranean region (Hurrell, 1995; Serreze et al., 1997; Dai et al., 1997; Mariotti et al., 2002; Mariotti and Arkin, 2007). The negative phase (especially that of MO, with higher anomalies in the SLP field) is linked to an intense cyclogenesis over the central/western Mediterranean that produces anomalously wet conditions over most of the basin and, hence, negative correlation with P. Precipitation anomalies during the positive and negative phases (higher and lower quartiles) of the indices are shown in Table 2. MO exerts the strongest influence with precipitation anomalies close to 100 mm/year on average over most of the basin. Higher anomalies are observed in the northern Mediterranean in both phases with values up to -200 mm/year during the positive phase in the Ionian and Levantine sub-basins and up to 250 mm/year during the negative phase in the Ionian and north Adriatic (see Figure 3C-D). All indices result in precipitation anomalies of similar sign across the basin (see Table 2), except the positive EA phase that produces a dipole response with positive (negative) anomalies in some areas of the eastern (western) basin.

Basin wide (Figure 3E), decadal to interdecadal variability of the Mediterranean precipitation appears to be even more closely related to NAO and MO indices with correlations of -0.82 and -0.76, respectively (Table 1). In particular, the decrease from mid-60s to early-90s corresponds to a switch from a low to a high state of the indices (notice that –NAO and -MO indices have been plotted). These results are in good agreement with those of Mariotti et al. (2002), who obtained (only for NAO) a correlation of -0.51 and -0.84 for annual and decadal (5-year running means) variability, respectively and confirms the importance of the choice of a long period for budget studies in the Mediterranean, since the long time scale effects of the indices must be taken into account because of their direct implication on the variables (Pettenuzzo et. al., 2010).

--------------------------------Approximate location of Table 2--------------------------------

3.2.- Evaporation

On annual basis, MO index presents also the strongest correlation (*r* = -0.36 on average, Table 1) with evaporation although only some areas of the Levantine (with stronger negative correlation, *r* close to -0.6) and western sub-basins are significantly correlated (Figure 4A). NAO performs a rather similar influence (*r* = 0.33 on average over 37% of the Mediterranean) whereas EA and EA-WR seem to be poorly correlated with evaporation. At decadal timescales (5-year running means), NAO and MO show the same correlation (*r* = 0.52 on average) although NAO affects more extensive areas, especially the Liguro-Provencal, south of Greece (with values close to -0.8) and Levantine sub-basins (Figure 4B). It is interesting to mention that the MO influence extends to almost 80% of the basin (with similar correlation values) if the summer index is considered. Since evaporation is higher in autumn (Mariotti et al., 2002; Romanou et al., 2010; Criado-Aldeanueva et al., 2012), it could be argued that the atmospheric forcing in summer pre-conditions to a certain extent its evolution in the following months. From 1979, higher correlation is observed for most indices, especially EA with *r* above 0.7 over more than 90% of the Mediterranean.

Anti-correlation for MO (and NAO) is again expected since, in its negative phase, anomalously low pressure over the whole basin is observed (see Figure 2H). This favors colder and dryer air masses from Central Europe generate more severe weather conditions over the northern and eastern Mediterranean and hence an intensification of evaporative losses to the atmosphere. Conversely, the positive MO phase is associated with higher than average pressure over the Mediterranean and North Africa (Figure 2G) that promote a shift of the wind trajectories toward lower latitudes. Warmer and moister air masses are then conveyed toward the Mediterranean leading to milder winters and a consequent decrease in the evaporative loss, similarly as showed by Hurrell (1995) for the NAO.

Negative evaporation anomalies are higher under the positive NAO phase (-92 mm/year on average over most of the basin, see Table 1) with values up to -160 mm/year in the Levantine basin and the Gulf of Lions (Figure 4C), two well documented sites of formation of Levantine Intermediate Water (LIW) and Western Mediterranean Deep Water (WMDW), respectively. This decrease in evaporation (and associated latent heat losses) may reflect in a reduction of the intermediate and deep waters formed (see Josey, 2003 and Papadopoulos et al., 2012b for a complete discussion of the winter convection processes). As for precipitation, the negative MO phase exerts stronger influence and leads to higher (positive) evaporation anomalies (98 mm/year on average, Table 1), with values above 400 mm/year in the Levantine sub-basin (Figure 4D). In this phase, the dipole of anomalously low pressure over Central Europe and Turkey (Figure 2H) brings colder and dryer air masses from continental regions to the Levantine sub-basin that enhance evaporative losses in this area and may promote winter LIW formation. All indices result in evaporation anomalies of similar sign across the basin (see Table 2), except the EA-WR pattern that produces a dipole response with positive (negative) anomalies in most of the eastern (western) basin in the positive phase and vice-versa that will be commented in detailed for the net heat flux.

--------------------------------Approximate location of Figure 4--------------------------------

Basin wide (Figure 4E), decadal to interdecadal variability of the Mediterranean evaporation is well correlated with the NAO index (r = -0.6, Table 1) but not significantly with EA or EA-WR (in case of EA-WR because it produces correlation of different sign in the eastern and western sub-basins). Correlation increases from 1979 (ERA-Interim, $NCEP_{79\text{-}09}$) and a very good agreement between the EA time series and basin-averaged evaporation (Figure 4E) is found (r = 0.87 and 0.7, respectively). However, this increase is more likely to be related to the shorter period analysed, that has coincided with an agreement of both time series in contrast to the departure observed before 1979.

3.3.- E – P freshwater budget

The freshwater budget E-P is the combination of the two above contributions E and P. On annual basis, MO index gives correlation of different sign in the easternmost Levantine sub-basin (negative correlation up to -0.4) and some areas of the Adriatic, the Ionian, the Aegean and the western sub-basin near Corsica and Sardinia (positive correlation up to 0.8, Figure 5A). However, only 38% of the Mediterranean is significantly correlated with this index (Table 1). The spatial pattern correlation of EA is rather similar to that of MO (r = 0.35 on average) whereas NAO and EA-WR are not significantly correlated in most of the basin. From 1979, the correlation with all climatic indices tends to increase but the fraction of points significantly correlated is lower. At decadal timescales (5-year running means), this bi-modal pattern becomes more evident with significant positive correlation almost everywhere (higher values up to 0.8 in the Adriatic and north Ionian) and negative correlation restricted to the easternmost Levantine sub-basin (Figure 5B for EA and similarly for MO and NAO, the latter with lower correlation values). For the recentmost decades, a fairly good correlation is found with EA (*r* = 0.7 on average from ERA-Interim data over more than 70% of the basin).

E-P anomalies under the positive and negative phases of the indices also follow this bi-modal pattern as a consequence of the different sensitiveness of E and P to the atmospheric forcing in each region. Again, the negative phase of MO index exerts the strongest influence (Table 2), with positive anomalies up to 400 mm/year in the Levantine sub-basin and negative anomalies about -200 mm/year above 35ºN (Figure 5C). As shown in Figures 3-4D, the negative phase of MO is associated with intense (positive) evaporation anomalies and a minor increase in precipitation in the Levantine basin that result in this E-P pattern. In contrast, north of 35ºN, the noticeable precipitation increase (Figure 3D) and the reduced changes in evaporation (Figure 4D) result in a negative E-P anomaly (Figure 5C). Opposite conditions prevail during the positive MO phase: negative anomalies in the Levantine basin and positive north of 35ºN (not shown), with more moderate values (Table 2). A rather similar spatial pattern is observed for NAO (see Table 2 for average values) but the fraction of points significantly influenced is lower. EA-WR also affects E-P in a dipolar manner but in this case E is dominant and changes in E-P closely follow those of E (positive/negative anomalies in some areas of the eastern/western basin in the positive phase and vice-versa). The only exception to this bi-modal pattern is associated to the negative EA phase that produces negative E-P anomalies in most of the basin (Figure 5D). In this state, precipitation anomalies are higher than those of evaporation except in the Levantine and north western sub-basins, where they tend to compensate and result in non-significant E-P changes (Figure 5D).

--------------------------------Approximate location of Figure 5--------------------------------

Mediterranean-averaged decadal to interdecadal E-P variability (Figure 5E) is not significantly correlated with MO, NAO and EA-WR due to this bi-modal pattern of correlation of opposite sign. EA shows a reasonably good correlation (r = 0.59, Table 2) that increases if only the period from 1979 is considered (r = 0.85 from ERA-Interim data) because the 60s decade of high discrepancy has been left out.

3.4.- Net heat flux

The net air-sea heat flux is the sum of the two radiation components (solar shortwave radiation absorbed by the sea and longwave radiation emitted by the sea) and the two turbulent terms (latent and sensible heat). Annual net heat flux is moderately correlated (r close to 0.4 on average, Table 1) with MO index (Figure 6A) in most parts of the Mediterranean (except the Alboran, Adriatic and north Aegean sub-basins, where correlation is not significant). Similar results are found for NAO index but more extended areas (especially the southern Ionian, not shown) are not significantly correlated whereas for EA and EA-WR only ~25% of the basin is significantly correlated on annual basis (Table 1). Decadal variations (5-year running means) are more correlated with the atmospheric indices, especially with MO (r up to -0.9 off Sicily and south of Greece and close to -0.7 in most of the Levantine basin, Figure 6B).

As shown by Criado-Aldeanueva et al. (2012), the net heat flux variability is mostly determined by the latent heat variability, this contribution becoming the main source of interannual variability. Since latent heat is directly related to evaporation, similarity between Figures 4 and 6 (panels A-B) is expectable. However, stronger correlation is observed with NAO and MO for net heat flux (see also Table 1) due to the contribution of the other components that correlate well with these indices. Notice that the sign of the correlation is negative because we have selected net heat flux positive toward the atmosphere (the same as evaporation).

--------------------------------Approximate location of Figure 6--------------------------------

We can now compare these results with those of Papadopoulos et al. (2012b), who correlate latent and sensible heat fluxes (from OAFlux, Yu et al., 2008) with several climatic indices (the four of this study among others) during winter (November to March). For the net heat flux, we find on annual basis a higher correlation with NAO index (r = 0.37 on average compared to their ~0.2) and a minor fraction of points influenced by EA-WR (26% compared to their ~60%). They also report a positive correlation with MO index in the westernmost Balearic and Alboran sub-basins that has not been found on annual basis. But the most outstanding difference is related to EA pattern: on annual basis, only ~25% of the Mediterranean is significantly correlated with EA index (Table 1) but during winter its influence extends to most of the basin (with r up to 0.6) and plays a significant role in the heat loss associated to intermediate and deep water formation processes (Josey et al., 2011; Papadopoulos et al., 2012a, b). Despite the different datasets and time periods analysed, these changes are likely to be related to the seasonal variability of the EA pattern that is enhanced during wintertime and weakens in spring and summer (Barnston and Livezey, 1987; Rogers, 1990).

Negative net heat flux anomalies over the entire Mediterranean Sea are associated with the positive NAO and MO phases (Table 2), due to a higher shortwave radiation and lower sensible and, especially, latent losses (i.e. -2.5 Wm^{-2}, +1.2 Wm^{-2}, -2.9 Wm^{-2} and -7.2 Wm^{-2} for shortwave, longwave, sensible and latent terms respectively in the positive NAO phase). Opposite conditions prevail in the negative MO phase, with positive heat anomalies all across the basin mainly due to higher evaporative losses (5.4 Wm^{-2}, -3.4 Wm^{-2}, 2.2 Wm^{-2} and 6.9 Wm^{-2} for shortwave, longwave, sensible and latent terms respectively) that become more important in the Levantine basin (Figure 4D, an explanation for this is provided in section 3.2).

Since latent heat variability regulates the neat heat flux variability, the spatial patterns of net heat anomalies in the positive and negative NAO and MO phases are similar to those of evaporation (Figure 4C-D) and will not be repeated here. Instead, we will discuss now the influence of EA and EA-WR to compare with previous works that perform a similar analysis for wintertime. The negative EA phase (Figure 6D) is associated with positive net heat anomalies in the western basin (up to 8-10 Wm^{-2}) and some areas of the Levantine sub-basin with values higher than 8 Wm^{-2}. However, anomalies are significantly different from zero only in 54% of the Mediterranean and the spatially-averaged net heat anomaly is ~5 Wm^{-2} (Table 2). As shown in Figure 2D, in the negative EA phase higher than average SLPA over the British Islands induces north-easterly flow of cold dry air which steepens the sea-air temperature and humidity gradient, this favouring stronger than normal heat loss over the entire basin. The influence of EA pattern in enhanced heat losses is similar to that of NAO (~5.5 Wm^{-2} in 46% of the basin, Table 2) but both are less than half of MO. Josey et al. (2011) found a stronger effect of EA pattern in winter heat losses and a minor impact of NAO (they did not considered the MO pattern). Since they also analysed NCEP dataset in a similar time period (1958-2006), differences are likely to be attributable to the seasonality of the atmospheric patterns. The enhanced EA high (in its negative state) and a slight shift to the east during winter may lead to a much stronger influence over the whole basin in this season.

EA-WR mode generates net heat anomalies of opposite sign in the eastern and western sub-basins. In its positive state, positive anomalies (mainly associated to higher latent losses) are found in the eastern sub-basin with values up to 15 Wm^{-2} in the Levantine area whereas negative anomalies (due to lower latent losses) locate in the Adriatic and Balearic sub-basin with more moderate values (~ 5 Wm^{-2}). This dipolar pattern can be explained based on the SLPA associated to the positive EA-WR phase (Figure 2E): the higher than average SLPA over north Europe induces a northerly flow of cold dry air over the eastern basin but a southerly flow of relatively warm moist air over the western basin leading to net heat anomalies of different sign. Opposite conditions prevail during the negative phase and thus, variations in the sign of EA-WR have the potential to induce see-saw variations in the heat budgets of the eastern and western basins, as shown by Josey et al. (2011), who found a strong impact of this mode in winter heat fluxes.

Basin wide (Figure 6E), decadal to interdecadal Mediterranean net heat flux variability is well correlated with NAO and MO indices (r = -0.68 and -0.63, respectively). As previously said, the bimodal pattern associated to EA-WR prevents a good correlation when Mediterranean-averaged net heat is considered. Similarly as for evaporation (remind this term is the main source of interannual net heat variability), a very good correlation with EA is found from 1979 (r = 0.83 from ERA-Interim and 0.69 from $NCEP_{79\text{-}09}$, see also Figure 6E).

4.- SUMMARY AND CONCLUDING REMARKS

We have correlated interannual to interdecadal precipitation, evaporation, freshwater budget (E-P) and net heat flux with the climatic indices NAO, EA, EA-WR and MO to explore the influence of atmospheric forcing in the Mediterranean freshwater and heat budgets variability. A composite analysis to highlight the differences between the positive and negative phases of the indices and hence, to determine the cause-effects relationships between them has also been performed. Although NAO and MO show in general a similar influence on the Mediterranean, some differences are worth mentioning: i) on annual basis, MO index gives the highest correlation with all the variables considered (Table 1); ii) particularly during its negative phase, MO exerts a stronger influence than NAO and is associated with higher precipitation and, especially, evaporative losses in the Levantine basin.

Both NAO and MO induce precipitation anomalies of the same sign all across the basin and the Mediterranean-averaged precipitation decrease from mid-60s to early-90s clearly corresponds to a switch from a negative to a positive phase of both indices. For evaporation, their influence is more pronounced in the Levantine basin, with positive anomalies (and associated latent heat losses) during the negative phase. Precisely, the different sensitiveness of E and P across the Mediterranean leads to correlations of opposite sign for E-P in the easternmost area with respect to the rest of the basin. EA pattern does not significantly affect P in the Mediterranean but a high correlation is found for E and net heat from 1979 that is worth to be followed. The strong effect of this mode in winter heat losses reported by Josey et al. (2011) is not so evident on annual basis due to the seasonality of EA pattern that weakens in spring and summer (Barnston and Livezey, 1987; Rogers, 1990). In contrast, EA-WR mode plays a significant role generating net heat anomalies of opposite sign in the eastern and western sub-basins, as previously found by Josey et al. (2011).

To conclude, taking into account that MO is not independent from the other modes of low frequency variability (especially from NAO, $r = 0.57$ on annual basis), we have shown its potential to affect more intensely the variables over the Mediterranean Sea and provide a valuable measure of the atmospheric impact on the basin, then becoming a powerful tool for monitoring heat and freshwater budgets variability.

ACKNOWLEDGEMENTS

This work has been carried out in the frame of the P07-RNM-02938 Junta de Andalucia Spanish-funded project. JSN acknowledges a postgraduate fellowship from Conserjería de Innovación Ciencia y Empresa, Junta de Andalucía, Spain. Partial support from CTM2010-21229 (M. of Science and Technology) Spanish-funded project is also acknowledged. NCEP and CMAP data have been provided by the NOAA/OAR/ESRL PSD, Boulder, Colorado, USA, from their website at http://www.esrl.noaa.gov/psd/. ECMWF ERA-Interim data used in this study have been obtained from the ECMWF data server. Time series of the teleconnection patterns were retrieved from the NOAA Climate Prediction Centre. Comments of three anonymous reviewers were of great help to improve the former manuscript.

REFERENCES

Angelucci, M. G., N. Pinardi, and S. Castellari, 1998. Air–sea fluxes from operational analyses fields: Intercomparison between ECMWF and NCEP analyses over the Mediterranean area. Phys. Chem. Earth, 23, 569–574.

Barnston, A.G. and Livezey, R.E., 1987. Classification, seasonality and persistence of low-frequency atmospheric circulation patterns. Mon. Weather Rev. 115, 1083-1126.

Berrisford, P., Dee, D., Fielding, K., Fuentes, M., Kallberg, P., Kobayashi, S., Uppala, S., 2009. The ERA-Interim archive. ECMWF Technical Report 1, 20 pp.

Bethoux, J.P, 1979. Budgets of the Mediterranean Sea: their dependence on the local climate and on the characteristics of Atlantic waters. Ocean. Acta 2, 157-163.

Bethoux, J.P. and Gentili B., 1999. Functioning of the Mediterranean Sea: Past and Present Changes realed to freshwater input and climatic changes. J. Mar. Syst. (20), 33-47.

Boukthir, M., and B. Barnier, 2000. Seasonal and inter-annual variations in the surface freshwater flux in the Mediterranean Sea from the ECMWF re-analysis project. J. Mar. Syst., (24), 343–354.

Bryden, H. L., and T. H. Kinder, 1991b. Steady two-layer exchange through the Strait of Gibraltar. Deep-Sea Res., 38S, 445–463.

Bunker, A.F., Charnock, H., Goldsmith, R.A., 1982. A note on the heat balance of the Mediterranean and Red Seas. J. Mar. Res. 40, 73-84, Suppl.

Castellari, S., Pinardi, N., Leaman K., 1998. A model study of air-sea interactions in the Mediterranean Sea. J. Mar. Sys. 18, 89-114.

Conte, M., Giuffrida, A. and Tedesco, S., 1989. The Mediterranean Oscillation, impact on precipitation and hydrology in Italy. Conference on Climate Water. Pub. of the Academy of Finland, Helsinki, 121-137.

Criado-Aldeanueva, F., Soto-Navarro, J., García-Lafuente, J., 2012. Seasonal and interannual variability of surface heat and freshwater fluxes in the Mediterranean Sea: budgets and exchange through the Strait of Gibraltar. International Journal of Climatology, 32, 286-302 doi: 10.1002/joc.2268.

Dai, A., Fung, I.Y., del Genio, A.D., 1997. Surface observed global land precipitation variations during 1900-88. J. Clim 10, 2943-2962.

Garrett, C., Outerbridge, R., Thompson, K., 1993. Interannual variability in Mediterranean heat and buoyancy fluxes. J. Climate 6, 900-910.

Gilman, C., Garrett, C., 1994. Heat flux parameterization for the Mediterranean Sea: the role of atmospheric aerosols and constraints from the water budget. J. Geophys. Res. 99 (C3), 5119-5134.

Gomis, D., Tsimplis, M.N., Martín-Míguez, B., Ratsimandresy, A.W., García-Lafuente, J. and Josey, S.A., 2006. Mediterranean sea level and barotropic flow through the Strait of Gibraltar for the period 1958-2001 and reconstructed since 1659. J. Geophys. Res. 111, C11005 doi: 10.1029/2005JC003186.

Harzallah, A., D. L. Cadet, and M. Crepon, 1993. Possible forcing effects of net evaporation, atmospheric pressure and transients on water transports in the Mediterranean Sea. J. Geophys. Res., 98 (C7), 12 341–12 350.

Hurrell, J.W., 1995. Decadal trends in the North Atlantic Oscillation – regional temperatures and precipitation. Science 269(5224), 676-679.

Hurrell, J.W. and van Loon, H., 1997. Decadal variations in climate associated with the North Atlantic Oscillation. Clim. Change 36, 301-326.

Hurrell, J.W., Kushnir, Y., Ottersen, G. and Visbeck, M., 2003. The North Atlantic Oscillation: climate significance and environmental impact. Geophys. Monogr. Ser 134, 279pp.

Hurrell, J.W. and Deser, C., 2010. North Atlantic climate variability: the role of the North Atlantic Oscillation. J. Mar. Sys. 79, 231-244.

Jones, P.D., Jonsson, T. and Wheeler, D., 1997. Extension to the North Atlantic Oscillation using early instrument pressure observations from Gibraltar and south-west Iceland. Int. J. Climatol. 17, 1433-1450.

Jones, P.D., Osborn, T.J. and Briffa, K.R., 2003. Pressure-based measures of the North Atlantic Oscillation (NAO), a comparison and assessment of changes in the strength of the NAO and its influence on surface climate parameters. In: Hurrell, J.W., Kushnir, Y., Ottersen, G. and Visbeck, M (eds), The North Atlantic Oscillation, climatic significance and environmental impact. AGU Geophys. Monogr., vol. 134, pp 51-62.

Josey, S. A., 2003. Changes in the heat and freshwater forcing of the eastern Mediterranean and their Influence on deep water formation, Journal of Geophysical Research, 108(C7), 3237, doi:10.1029/2003JC001778.

Josey, S.A., Marsh, R., 2005. Surface freshwater flux variability and recent freshening of the North Atlantic in the Eastern Subpolar Gyre, J. Geophys. Res., 110, C05008, doi:10.1029/2004JC002521.

Josey, S.A., Somot, S., Tsimplis, M., 2011. Impacts of atmospheric modes of variability on Mediterranean Sea surface heat exchange. Journal of Geophysical Research 116, C02032 doi: 10.1029/2010JC006685.

Kalnay, E and co-authors (1996). The NCEP/NCAR 40-year reanalysis project. Bull. Amer. Meteor. Soc., 77:437-471.

Kutiel, H., Maheras, P. and Guika, S., 1996. Circulation indices over the Mediterranean and Europe and their relationship with rainfall conditions across the Mediterranean. Theor. Appl. Climatol. 54, 125-138.

van Loon, H. and Rogers, J.C., 1978. The see-saw of winter temperatures between Greenland and northern Europe. Part I: general descriptions. Mon. Weather Rev 106, 296-310.

Maheras, P., Xoplaki, E. and Kutiel, H., 1999. Wet and dry monthly anomalies across the Mediterranean basin and their relationship with circulation 1860-1990. Theor. Appl. Climatol 64, 189-199.

Mariotti, A., Struglia, M.V., Zeng, N., Lau, K.-M., 2002. The hydrological cycle in the Mediterranean region and implications for the water budget of the Mediterranean Sea. Journal of Climate 15, 1674–1690.

Mariotti, A. and Arkin, P., 2007. The North Atlantic Oscillation and oceanic precipitation variability. Clim. Dyn 28, 35-51.

Mariotti A, 2010. Recent Changes in the Mediterranean Water Cycle: A Pathway toward Long-Term Regional Hydroclimatic Change? Journal of Climate 23 (6), 1513-1525.

Matsoukas, C., Banks, A. C., Hatzianastassiou, N., Pavlakis, K. G., Hatzidimitriou, D., Drakakis, E., Stackhouse, P. W., Vardavas, I., 2005. Seasonal heat budget of the Mediterranean Sea. J. Geophys. Res., 110, C12008, doi:10.1029/2004JC002566.

May, P.W., 1986. A brief explanation of Mediterranean heat and momentum flux calculations. NORDA code 322, NSTL, MS 39529.

Palutikof, J.P., 2003: Analysis of Mediterranean climate data: measured and modelled. In: Bolle, H.J. (ed): Mediterranean climate: Variability and trends. Springer-Verlag, Berlin.

Papadopoulos, V., Kontoyiannis, H., Ruiz, S., Zarokanellos, N., 2012a. Influence of atmospheric circulation on turbulent air-sea heat fluxes over the Mediterranean Sea during winter. Journal of Geophysical Research 117, C03044, doi: 10.1029/2011JC007455.

Papadopoulos, V., Josey, S., Bartzokas, A., Somot, S., Ruiz, S., Drakopoulou, P., 2012b. Large-scale atmospheric circulation favoring deep –and intermediate- water formation in the Mediterranean Sea. Journal of Climate 25, 6079-6091.

Peixoto, J. P., M. De Almeida, R. D. Rosen, and D. A. Salstein, 1982. Atmospheric moisture transport and the water balance of the Mediterranean Sea. Water Resour. Res., 18, 83–90.

Pettenuzzo, D., Large, W.G. and Pinardi, N. (2010). On the corrections of ERA-40 surface flux products consistent with the Mediterranean heat and water budgets and the connection between basin surface total heat flux and NAO. J. Geophys. Res. 115, C06022, doi: 10.1029/2009JC005631.

Rogers, J.C. and van Loon, H., 1979. The see-saw of winter temperatures between Greenland and northern Europe. Part II: some oceanic and atmospheric effects in middle and high latitudes. Mon. Weather Rev 107, 509-519.

Rogers, J.C., 1984. The association between the North Atlantic Oscillation and the Southern Oscillation in the northern hemisphere. Mon. Weather Rev. 112 1999-2015.

Rogers, J.C., 1990. Patterns of low-frequency monthly sea-level pressure variability (1899-1986) and associated wave cyclone frequencies. Journal of Climate 3, 1364-1379.

Romanou, A., Tselioudis, G., Zerefos, C.S., Clayson, C.A., Curry, J.A., Anderson, A., 2010. Evaporation-preciptation variability over the Mediterranean and the Black Seas from satellite and reanalysis estimates. Journal of Climate 23, 5268-5287.

Ruiz S., Gomis D., Sotillo M. G., Josey S. A., 2008. Characterization of surface heat fluxes in the Mediterranean Sea from a 44-year high-resolution atmospheric data set. Global and Planetary change, (63), 256-274.

Serreze, M.C., Carse, F., Barry, R.G. and Rogers, J.C., 1997. Icelandic low cyclone activity: climatological features, linkages with the NAO and relationships with recent changes in the northern hemisphere circulation. J. Clim 10(3), 453-464.

Slonosky, V.C. and Yiou, P., 2001. Secular changes in the North Atlantic Oscillation and its influence on 20th century warming. Geophys. Res. Lett. 28, 807-810.

Supic, N., Grbec, B., Vilibic, I. and Ivancic, I., 2004. Long-term changes in hydrograpic conditions in northern Adriatic and its relationship to hydrological and atmospheric processes. Annales Geophysicae 22, 733-745.

Suselj, K. and Bergant, K., 2006. Mediterranean Oscillation Index. Geophys. Res. Abstr. 8, 02145 European Geosciences Union.

Trenberth, K.E., 1984. Signal versus noise in the Southern Oscillation. Mon. Weather Rev. 112, 326-332.

Walker, G.T. and Bliss, W.E., 1932. World Weather V. Memories of the Royal Meteorological Society 44, 53-84.

Xie P, Arkin PA. 1996. Analysis of global monthly precipitation using gauge observations, satellite estimates, and numerical model predictions. Journal of Climate **9**: 840–858.

Xie P, Arkin PA. 1997. Global precipitation: A 17-year monthly analysis based on gauge observations, satellite estimates, and numerical model outputs. Bulletin of the American Meteorological Society **78**: 2539–2558.

Yu, L., Jin, X. and Weller, R.A., 2008. Multidecade global flux datasets from the Objectively Analyzed Air-sea Fluxes (OAFlux) project: latent and sensible heat fluxes, ocean evaporation and related surface meteorological variables. OAFlux proj. Tech. Rep. OA-2008-01, 64pp. Woods Hole Oceanogr. Inst. Woods Hole, Mass.

FIGURE CAPTIONS

Table 1: Mean absolute correlation at 95% significance level between annual and decadal (5-years running means) climatic indices and P, E, E-P and net heat flux (Q). The fraction of grid points significantly correlated is shown in brackets. The last column displays the correlation (n.s. indicates that correlation is not significant) between the selected indices and the Mediterranean-averaged variables at decadal (5-years running means) timescale (time series of panel E in Figures 3-6). Boldface indicates the strongest influence.

Table 2: Mediterranean averaged anomalies in the 1948-2008 period during the positive (CA+, higher quartile) and negative (CA-, lower quartile) phases of the selected climatic indices (NAO, MO, EA and EA-WR). Units are mm/year for P, E and E-P and Wm^{-2} for Q. Anomalies of opposite sign across the basin are separated by /. The fraction

of points where the anomaly is significantly different from zero is shown in brackets. The spatial pattern of results highlighted in bold is shown in the corresponding figures.

Figure 1: Map of the Mediterranean Sea. The main basins and sub-basins are indicated.

Figure 2: Composites of sea level pressure anomalies (mbar) in the 1948-2008 period during the positive (higher quartile, left column) and negative (lower quartile, right column) phases of the selected climatic indices: A-B) NAO; C-D) EA; E-F) EA-WR; G-H) MO.

Figure 3: A) Correlation (95% significance) between annual precipitation (P) and MO index for the period 1948-2008. B) Correlation (95% significance) between 5-year running means P and MO index for the period 1948-2008. C) Composite of P anomalies (mm/year) under the positive (higher quartile) phase of MO index. D) Composite of P anomalies (mm/year) under the negative (lower quartile) phase of MO index. E) Time series of 5-year running means of Mediterranean-averaged P and the most correlated NAO and MO climatic indices.

Figure 4: A) Correlation (95% significance) between annual evaporation (E) and MO index for the period 1948-2008. B) Correlation (95% significance) between 5-year running means E and NAO index for the period 1948-2008. C) Composite of E anomalies (mm/year) under the positive (higher quartile) phase of NAO index. D) Composite of E anomalies (mm/year) under the negative (lower quartile) phase of MO index. E) Time series of 5-year running means of Mediterranean-averaged E and the selected NAO, MO and EA climatic indices.

Figure 5: A) Correlation (95% significance) between annual freshwater budget (E-P) and MO index for the period 1948-2008. B) Correlation (95% significance) between 5-year running means E-P and EA index for the period 1948-2008. C) Composite of E-P anomalies (mm/year) under the negative (lower quartile) phase of MO index. D) Composite of E-P anomalies (mm/year) under the negative (lower quartile) phase of EA index. E) Time series of 5-year running means of Mediterranean-averaged E-P and the most correlated EA climatic index.

Figure 6: A) Correlation (95% significance) between annual net heat flux (Q) and MO index for the period 1948-2008. B) Correlation (95% significance) between 5-year running means Q and MO index for the period 1948-2008. C) Composite of Q anomalies (Wm^{-2}) under the positive (higher quartile) phase of EA-WR index. D) Composite of Q anomalies (Wm^{-2}) under the negative (lower quartile) phase of EA index. E) Time series of 5-year running means of Mediterranean-averaged Q and the selected NAO, MO and EA climatic indices.

	Annual means				**5-years means**				**5-years Med-averaged**			
	NAO	**MO**	**EA**	**EA/WR**	**NAO**	**MO**	**EA**	**EA/WR**	**NAO**	**MO**	**EA**	**EA/WR**
P_{NCEP}	0.31 (33%)	**0.45 (56%)**	0.37 (35%)	0.31 (3%)	0.55 (87%)	**0.56 (81%)**	0.50 (55%)	0.39 (35%)	**-0.82**	-0.76	-0.43	n.s
P_{ERA-I}	0.42 (12%)	0.46 (21%)	n.s	0.41 (7%)	0.61 (42%)	0.57 (37%)	0.54 (37%)	0.57 (39%)	-0.57	-0.49	n.s	-0.40
P_{79-09}	0.41 (22%)	0.42 (26%)	0.40 (6%)	n.s	0.62 (81%)	0.54 (56%)	0.65 (74%)	0.54 (60%)	-0.74	-0.54	0.79	-0.56
P_{CMAP}	0.47 (31%)	0.51(26%)	0.44 (4%)	0.39 (4%)	0.61 (57%)	0.60 (40%)	0.54 (40%)	0.56 (21%)	-0.77	-0.60	n.s	n.s
E_{NCEP}	0.33 (37%)	**0.36 (40%)**	0.32 (10%)	0.33 (21%)	**0.52 (79%)**	0.52 (56%)	0.42 (49%)	0.45 (42%)	**-0.60**	-0.45	n.s	n.s
E_{ERA-I}	0.40 (15%)	0.40 (4%)	0.45 (24%)	0.42 (28%)	0.59 (89%)	0.50 (58%)	0.74 (91%)	0.57 (64%)	-0.68	-0.50	0.87	-0.53
E_{79-09}	0.42 (44%)	0.38 (5%)	0.45 (15%)	0.41 (13%)	0.63 (86%)	0.48 (56%)	0.64 (95%)	0.48 (31%)	-0.65	-0.41	0.70	n.s
$E-P_{NCEP}$	0.30 (15%)	**0.39 (38%)**	0.35 (33%)	0.33 (23%)	0.42 (59%)	0.48 (59%)	**0.51 (65%)**	0.42 (42%)	n.s	n.s	**0.59**	n.s
$E-P_{ERA-I}$	0.41 (13%)	0.44 (10%)	0.42 (6%)	0.44 (9%)	0.55 (61%)	0.53 (32%)	0.70 (72%)	0.54 (44%)	-0.46	n.s	0.85	-0.37
$E-P_{79-09}$	0.43 (17%)	0.43 (8%)	0.41 (9%)	0.41 (6%)	0.57 (44%)	0.55 (19%)	0.62 (55%)	0.54 (49%)	n.s	n.s	0.68	n.s
Q_{NCEP}	0.37 (51%)	**0.37 (59%)**	0.31 (24%)	0.36 (26%)	0.58 (76%)	**0.58 (83%)**	0.40 (49%)	0.52 (43%)	**-0.68**	-0.63	n.s	0.39
Q_{ERA-I}	0.41 (22%)	0.39 (4%)	0.42 (20%)	0.43 (34%)	0.58 (79%)	0.51 (44%)	0.68 (83%)	0.58 (66%)	-0.70	-0.51	0.83	-0.56
Q_{79-09}	0.46 (54%)	0.41 (6%)	0.44 (13%)	0.43 (17%)	0.64 (95%)	0.49 (54%)	0.65 (86%)	0.50 (21%)	-0.65	-0.41	0.69	n.s

Table 1: Mean absolute correlation at 95% significance level between annual and decadal (5-years running means) climatic indices and P, E, E-P and net heat flux (Q). The fraction of grid points significantly correlated is shown in brackets. The last column displays the correlation (n.s. indicates that correlation is not significant) between the selected indices and the Mediterranean-averaged variables at decadal (5-years running means) timescale (time series of panel E in Figures 3-6). Boldface indicates the strongest influence.

	NAO		MO		EA		EA/WR	
	CA +	CA -	CA +	CA -	CA +	CA -	CA +	CA -
P_{NCEP}	-83.1 (85%)	58.3 (62%)	**-93.0 (91%)**	**86.9 (78%)**	87.8/-39.4 (65%)	58.8 (79%)	37.6 (37%)	46.1 (49%)
E_{NCEP}	**-91.7 (92%)**	46.6 (41%)	-68.1 (78%)	**98.1 (74%)**	79.2 (81%)	37.3 (53%)	66.2/-36.4 (59%)	43.7/-78.3 (59%)
$E\text{-}P_{NCEP}$	74.3/-74.2 (63%)	57.4/-90.5 (51%)	75.1/-58.2 (73%)	**119.7/-89.3 (79%)**	88.2/-81.1 (77%)	**-65.7 (67%)**	60.8/-47.7 (49%)	51.4/-78.8 (45%)
Q_{NCEP}	-11.4 (91%)	5.5 (46%)	-8.4 (86%)	11.1 (86%)	8.1/-5.9 (67%)	**4.9 (54%)**	**9.4/-3.8 (70%)**	5.7/-10.1 (74%)

Table 2: Mediterranean averaged anomalies in the 1948-2008 period during the positive (CA+, higher quartile) and negative (CA-, lower quartile) phases of the selected climatic indices (NAO, MO, EA and EA-WR). Units are mm/year for P, E and E-P and Wm^{-2} for Q. Anomalies of opposite sign across the basin are separated by /. The fraction of points where the anomaly is significantly different from zero is shown in brackets. The spatial pattern of results highlighted in bold is shown in the corresponding figures.

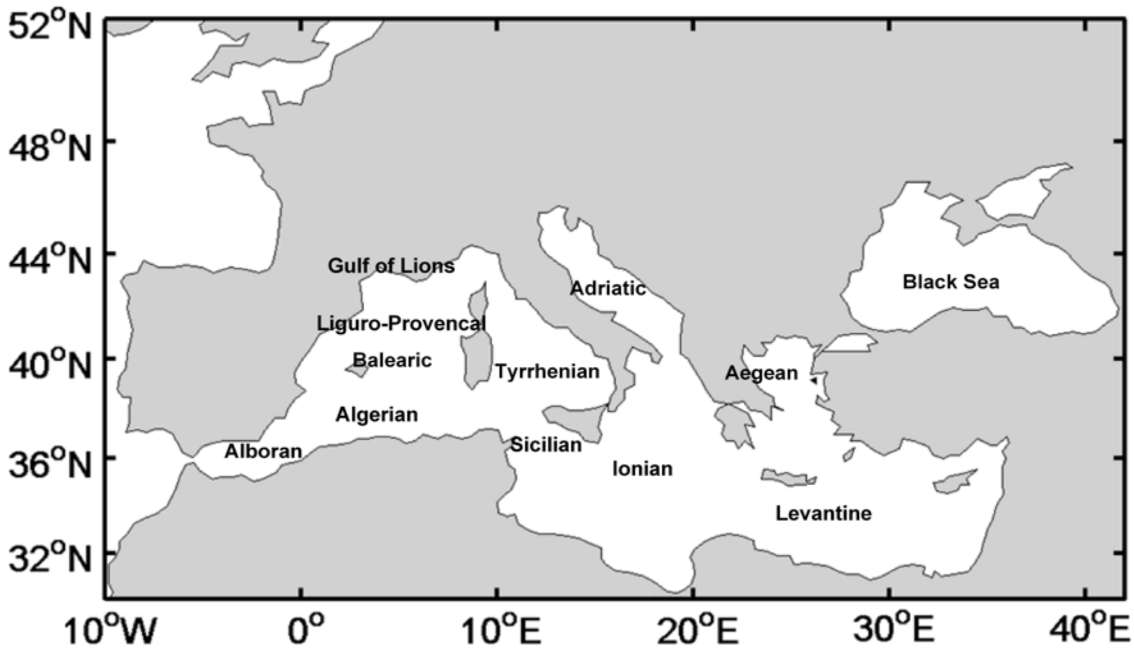

Figure 1: Map of the Mediterranean Sea. The main basins and sub-basins are indicated.

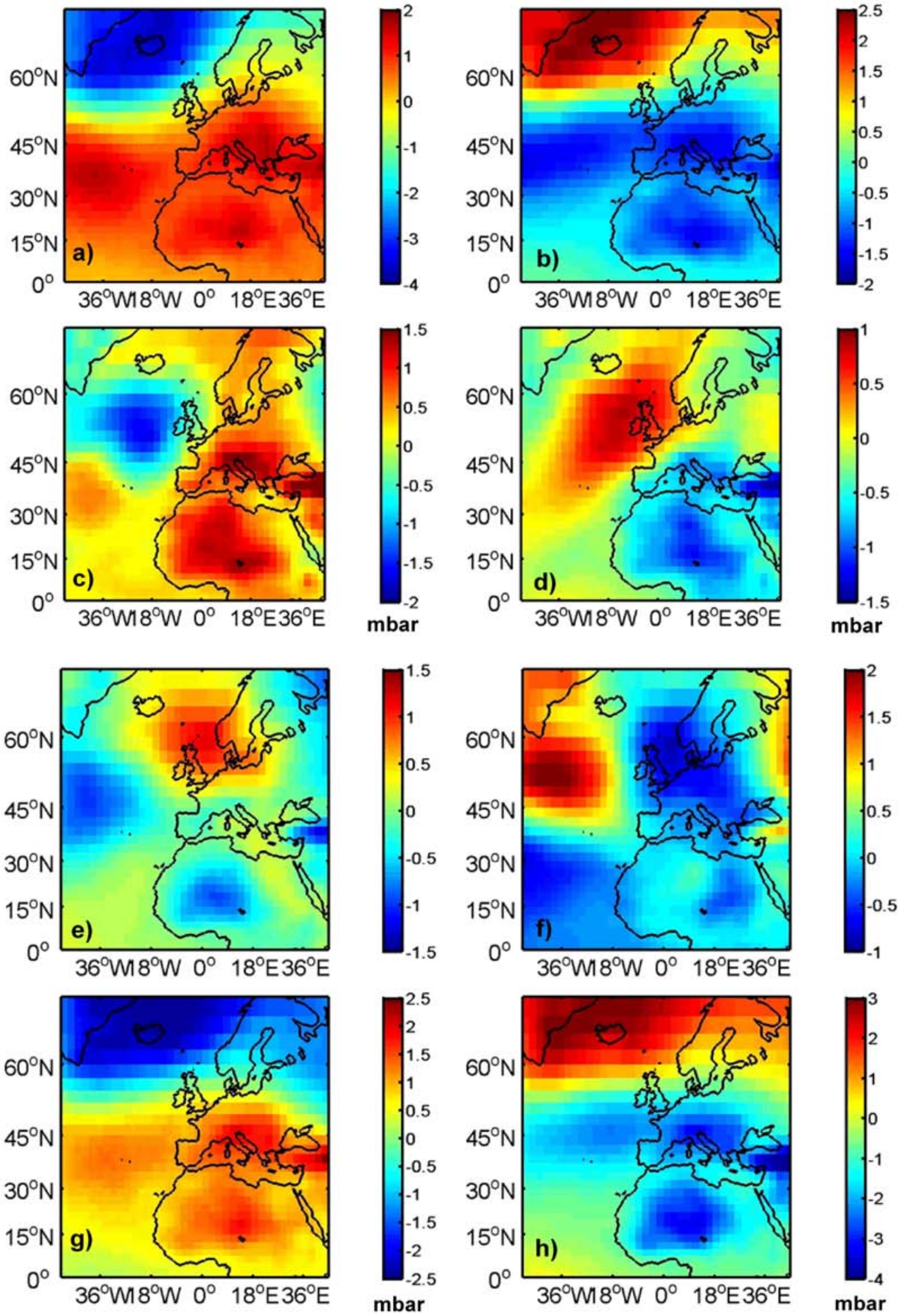

Figure 2: Composites of sea level pressure anomalies (mbar) in the 1948-2008 period during the positive (higher quartile, left column) and negative (lower quartile, right column) phases of the selected climatic indices: A-B) NAO; C-D) EA; E-F) EA-WR; G-H) MO.

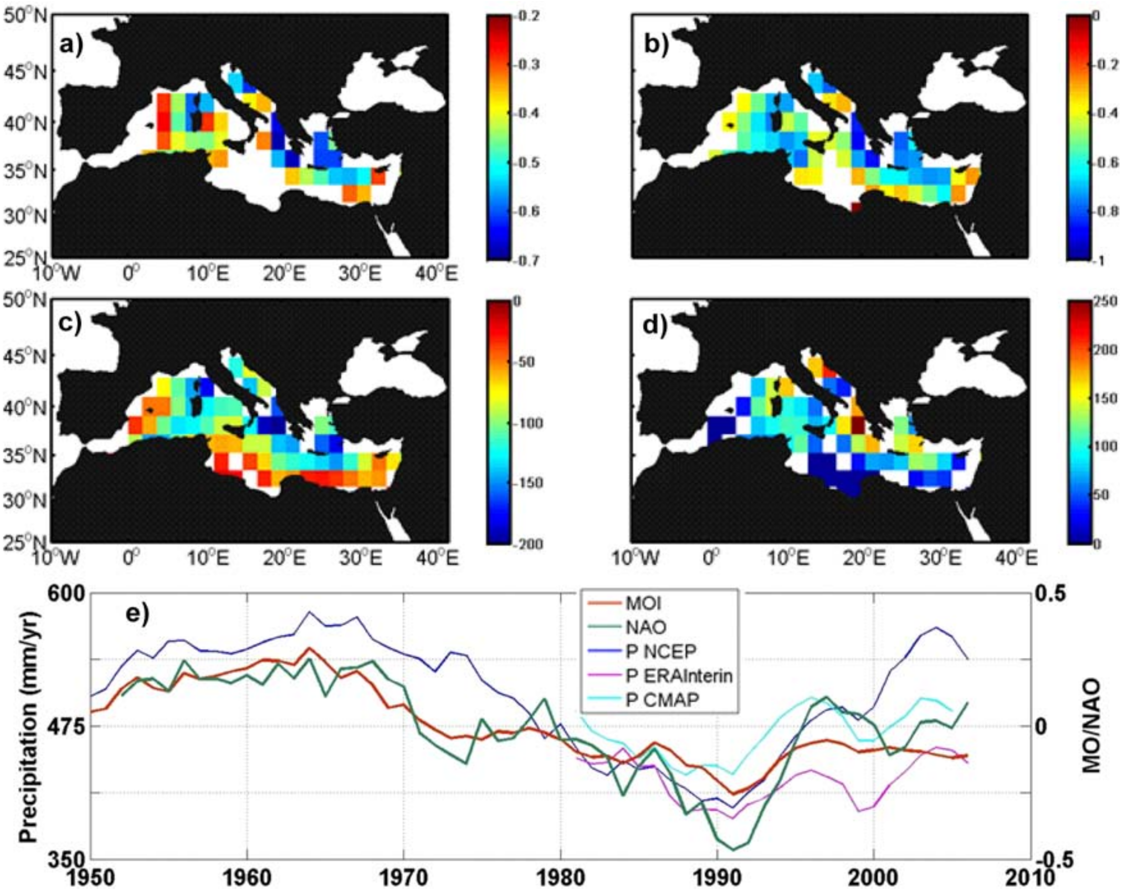

Figure 3: A) Correlation (95% significance) between annual precipitation (P) and MO index for the period 1948-2008. B) Correlation (95% significance) between 5-year running means P and MO index for the period 1948-2008. C) Composite of P anomalies (mm/year) under the positive (higher quartile) phase of MO index. D) Composite of P anomalies (mm/year) under the negative (lower quartile) phase of MO index. E) Time series of 5-year running means of Mediterranean-averaged P and the most correlated NAO and MO climatic indices.

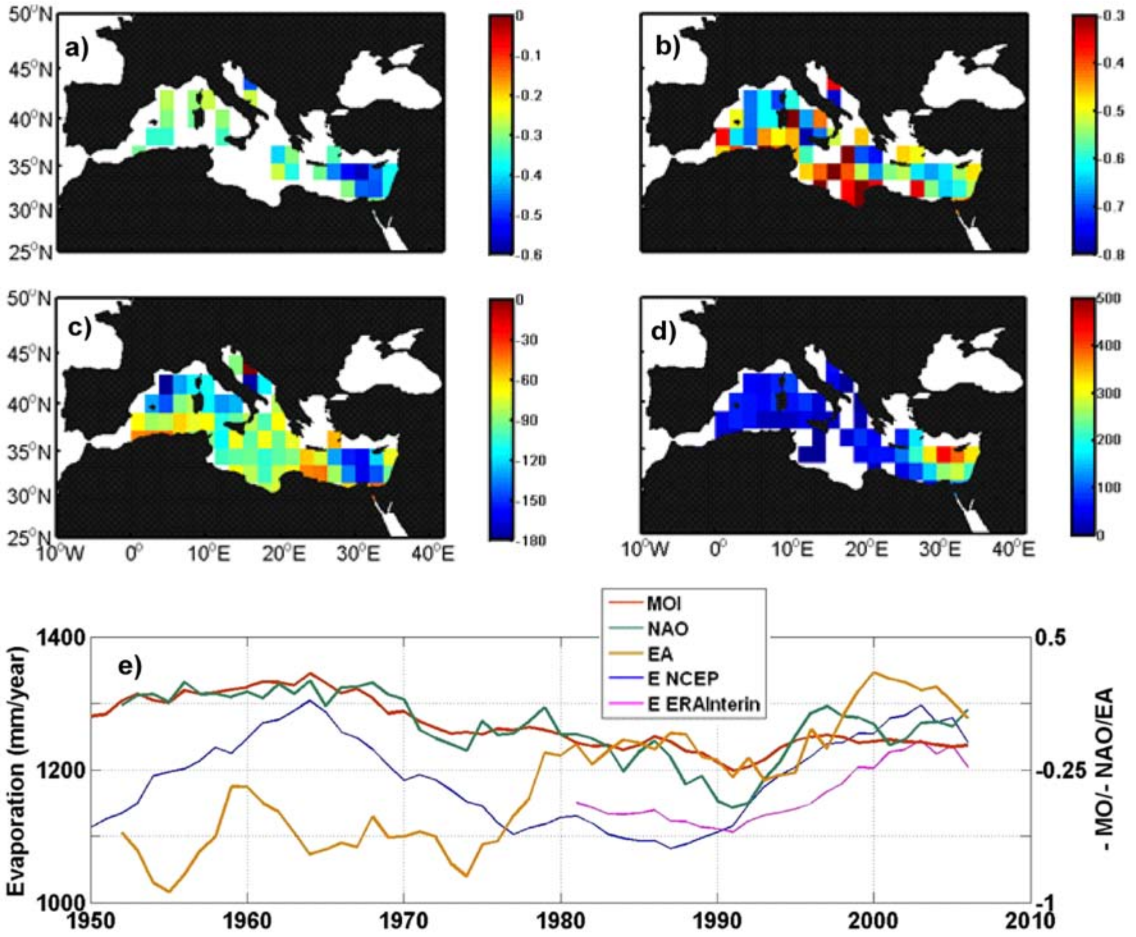

Figure 4: A) Correlation (95% significance) between annual evaporation (E) and MO index for the period 1948-2008. B) Correlation (95% significance) between 5-year running means E and NAO index for the period 1948-2008. C) Composite of E anomalies (mm/year) under the positive (higher quartile) phase of NAO index. D) Composite of E anomalies (mm/year) under the negative (lower quartile) phase of MO index. E) Time series of 5-year running means of Mediterranean-averaged E and the selected NAO, MO and EA climatic indices.

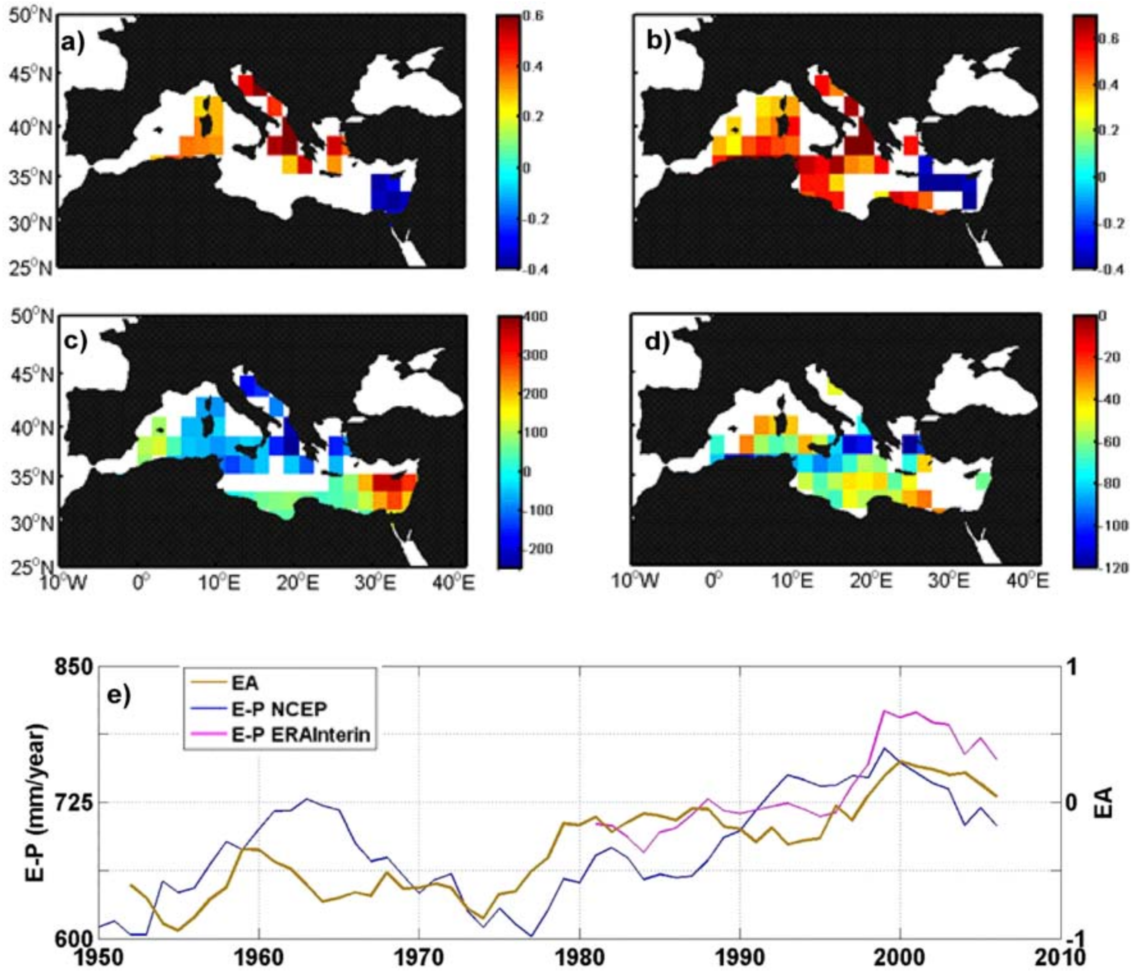

Figure 5: A) Correlation (95% significance) between annual freshwater budget (E-P) and MO index for the period 1948-2008. B) Correlation (95% significance) between 5-year running means E-P and EA index for the period 1948-2008. C) Composite of E-P anomalies (mm/year) under the negative (lower quartile) phase of MO index. D) Composite of E-P anomalies (mm/year) under the negative (lower quartile) phase of EA index. E) Time series of 5-year running means of Mediterranean-averaged E-P and the most correlated EA climatic index.

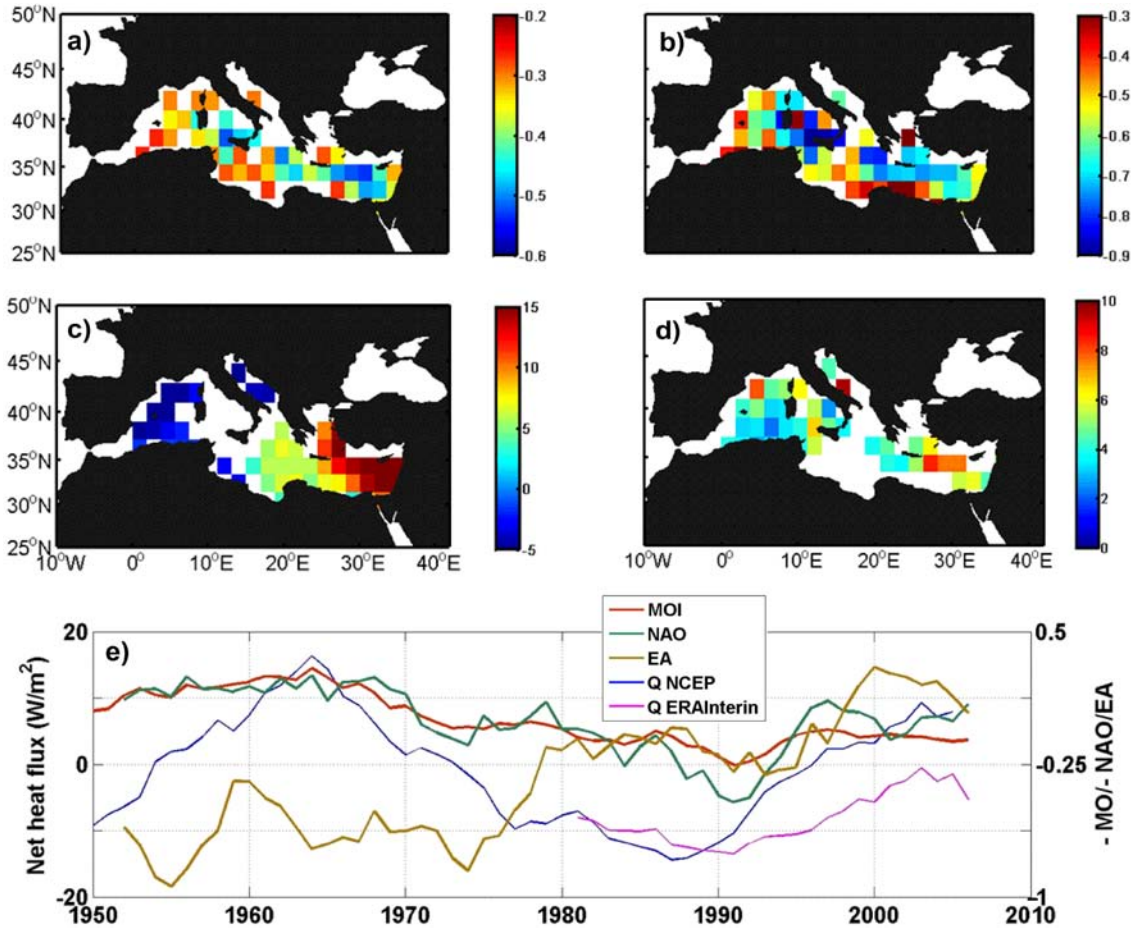

Figure 6: A) Correlation (95% significance) between annual net heat flux (Q) and MO index for the period 1948-2008. B) Correlation (95% significance) between 5-year running means Q and MO index for the period 1948-2008. C) Composite of Q anomalies (Wm^{-2}) under the positive (higher quartile) phase of EA-WR index. D) Composite of Q anomalies (Wm^{-2}) under the negative (lower quartile) phase of EA index. E) Time series of 5-year running means of Mediterranean-averaged Q and the selected NAO, MO and EA climatic indices.